Synthesis Mechanisms of Poly[styrene-*co*-(acrylic acid)]-Supported $TiCl_4$ Catalysts Modified by Magnesium Compounds

Du Lijun, Ye Jian, Wang Jingdai, Jiang Binbo, Yang Yongrong

Department of Chemical and Biochemical Engineering, State Key Laboratory of Chemical Engineering, Zhejiang University, Hangzhou 310027, People's Republic of China

Received 13 February 2011; accepted 30 April 2011
DOI 10.1002/app.34822
Published online 25 August 2011 in Wiley Online Library (wileyonlinelibrary.com).

ABSTRACT: Soluble poly[styrene-*co*-(acrylic acid)] (PSA) modified by magnesium compounds was used to support $TiCl_4$. For ethylene polymerization, four catalysts were synthesized, namely PSA/$TiCl_4$, PSA/$MgCl_2$/$TiCl_4$, PSA/(*n*-Bu)MgCl/$TiCl_4$, and PSA/(*n*-Bu)$_2$Mg/$TiCl_4$. The catalysts were characterized by a set of complementary techniques including X-ray photoelectron spectroscopy, Fourier-transform infrared spectroscopy, X-ray diffraction, thermogravimetric analysis, scanning electron microscopy, and element analysis. Synthesis mechanisms of polymer-supported $TiCl_4$ catalysts were proposed according to their chemical environments and physical structures. The binding energy of Ti 2p in PSA/$TiCl_4$ was extremely low as $TiCl_4$ attracted excessive electrons from —COOH groups. Furthermore, the chain structure of PSA was destroyed because of intensive reactions taking place in PSA/$TiCl_4$. With addition of (*n*-Bu)MgCl or (*n*-Bu)$_2$Mg, —COOH became —COOMg- which then reacted with $TiCl_4$ in synthesis of PSA/(*n*-Bu)MgCl/$TiCl_4$ and PSA/(*n*-Bu)$_2$Mg/$TiCl_4$. Although $MgCl_2$ coordinated with —COOH first, $TiCl_4$ would substitute $MgCl_2$ to coordinate with —COOH in PSA/$MgCl_2$/$TiCl_4$. Due to the different synthesis mechanisms, the four polymer-supported catalysts correspondingly showed various particle morphologies. Furthermore, the polymer-supported catalyst activity was enhanced by magnesium compounds in the following order: $MgCl_2$ > (*n*-Bu)MgCl > (*n*-Bu)$_2$Mg > no modifier. © 2011 Wiley Periodicals, Inc. J Appl Polym Sci 123: 2517–2525, 2012

Key words: polymer-supported catalyst; chemical environment; synthesis mechanisms; ethylene polymerization

INTRODUCTION

Since Chirkov created metal complexes immobilized on polymer supports, various functionalized polymer materials have been investigated to be supports of catalysts,[1,2] such as Ziegler-Natta catalysts for olefin polymerization.[3,4] The side effects of inorganic support could be eliminated by using polymers as support of Ziegler-Natta catalysts.

From the aspect of practical application, it is a challenge to anchor transition-metal complex onto a polymer support by a simple synthetic procedure and with minimum alteration of the ligand environments. In general, the presence of functional groups in the polymer structure is fundamental to promote chemical interactions between the catalyst and the support.[5] However, direct attachment of transition metals to the functional groups has negative effects on the performance of polymer-supported Ziegler-Natta catalysts. Magnesium compounds are often used to modify the polymer supports with an aim to optimize the performance of polymer-supported catalyst. Sun et al.[6,7] synthesized various polymer-supported Ziegler-Natta catalysts and conducted a preliminary investigation. They provided multiple hypotheses of the reaction mechanism based only on the kinetic curves of ethylene polymerization. No characterizations of catalysts and polymer were offered. Mteza et al.[8] supported $TiCl_4$ on a polyethylene-based copolymer with dual functional groups for ethylene polymerization. They prepared several catalysts under varied conditions to optimize the catalyst performance and provided a plausible theory for interpretation of the modifiers role. Schuchardt and coworkers[9] synthesized chlorinated organic polymers-supported $TiCl_4$ without any modification. They focused on the ethylene polymerization behavior of the catalysts.

Despite numerous efforts, the question regarding how the coordination between polymer support and transition metals affects the chemical environment as well as the ethylene polymerizations still has not

Correspondence to: J. Binbo (jiangbb@zju.edu.cn).
Contract grant sponsor: Project of National Natural Science Foundation of China; contract grant number: 21076180.
Contract grant sponsor: Fundamental Research Funds for the Central Universities; contract grant number: 2009QNA4028.

been definitively answered. Actually, the coordination effects are essential to the performance of polymer-supported catalysts. According to the Fourier-transform infrared spectroscopy (FTIR) results, Kaur et al.[10] concluded that $TiCl_4$ was coordinated with potential Lewis base sites, such as oxygen of carbonyl group and OCH_3 group on poly(methyl acrylate-*co*-1-octene). The surface chemical environment around polymer functional groups or Ti atoms was not analyzed.

Functional polystyrene is a kind of versatile support material for catalysts.[11–13] Researchers usually use linked polystyrene beads to support active catalysts. The homogeneous distribution of active sites is difficult to achieve due to the limitation of diffusion inside the polymer particles.[14] In our study, gel immobilized system was adopted for efficient utilization of the entire polymer support with active centers fixed on it.[15] Soluble poly[styrene-*co*-(acrylic acid)] (PSA) used here can swell or dissolve in solvents. Therefore, the magnesium compounds and catalytically active centers appear not only at the polymer surface but also in the bulk.[15,16] Furthermore, the potential to modify the polymer supports, especially the functional groups, provides an opportunity to directly investigate the influence of the chemical environments of the support on the olefin polymerization process.[11,17]

We modified the soluble PSA by several magnesium reagents, including magnesium chloride ($MgCl_2$), *n*-butylmagnesium chloride [(*n*-Bu)MgCl)], and di-*n*-butyl- magnesium [$(n\text{-Bu})_2Mg$]. Gel polymer was formed in the addition of magnesium compounds. $TiCl_4$ was then anchored on this gel polymer. Nonpolar solvent (*n*-hexane) was added in the gel system to precipitate the PSA-supported catalysts. Polymer-supported catalyst powders were obtained after drying. For characterization of the catalysts, X-ray photoelectron spectroscopy (XPS), FTIR, X-ray diffraction (XRD), X-ray scanning electron microscopy (SEM), thermogravimetric analysis (TGA), and element analysis were used. We sought to find the synthesis mechanisms of polymer-supported $TiCl_4$ catalysts modified by various magnesium reagents. In addition, ethylene polymerizations were conducted to provide insight into the influence of synthesis mechanisms on catalyst activity.

EXPERIMENTAL

Materials

All chemicals were manipulated under an inert atmosphere using standard Schlenk technique. High-purity nitrogen, polymerization-grade ethylene, and hydrogen were obtained from Sinopec Shanghai Corporation (Shanghai, China) and purified by sequentially passing them through copper catalyst column and alumina column. Solvents (heptane, hexane, tetrahydrofuran, and toluene) were dried over 4 Å molecular sieves for at least 10 days and then purified by solvent purification system of Innovative Technology. Magnesium chloride ($MgCl_2$, 97.5% wt, H_2O—2% max), (*n*-Bu)MgCl (20 wt % solution in THF/toluene), $(n\text{-Bu})_2Mg$ (1.0*M* solution in heptane) and titanium (IV) chloride ($TiCl_4$, ≥98.0% wt) were used as received from J&K Company, China. Triethylaluminium (TEA) was purchased from Aldrich, China. PSA provided by Changchun Institute of Applied Chemistry, Chinese Academy of Science, was dried at 70°C under nitrogen flow for 24 h before use. The average molecular weight of PSA was 19,225, containing 3.5 mmol —COOH/g PSA.

TABLE I
The Composition of the Four Catalysts

Components	Name	Mg (wt %)	Ti (wt %)	Mg/Ti molar ratio
$PSA/TiCl_4$	PT	0	0.10	0
$PSA/MgCl_2/TiCl_4$	PMT	2.70	3.44	1.54
PSA/(*n*-Bu)MgCl/$TiCl_4$	PB1T	1.39	1.66	1.64
PSA/$(n\text{-Bu})_2Mg/TiCl_4$	PB2T	2.58	5.96	0.84

Synthesis of polymer-supported catalysts

We used the same type of agitator and the same speed for well stirring in all experiments of preparing catalysts. PSA (7.50 g) were dissolved in THF solution (150.0 mL) and stirred for 2 h at 60°C, to prepare PSA/THF solution (0.05 g/mL). PSA/toluene solution of 0.05 g/mL was also prepared by dissolving 5.00 g PSA in 100.0 mL toluene. Four catalysts, shown in Table I, were synthesized by varying the modification reagents.

$PSA/TiCl_4$ catalyst

PSA/THF (40.0 mL) solution in a Schlenk flask (150 mL) was stirred at 0°C for 30 min. $TiCl_4$ (0.70 mL) was slowly added into the PSA solution by dropwise at 0°C. The mixture was stirred for 2 h, and then *n*-hexane (40.0 mL) was added into the mixture. The generated solid was precipitated. The mixture was decanted and washed by hexane for several times until the liquid was colorless. The residual solid was dried under vacuum at room temperature for 4 h.

$PSA/MgCl_2/TiCl_4$ catalyst

$MgCl_2$ (0.42 g) was added into PSA/THF solution (26.0 mL) in a Schlenk flask (150 mL), stirred at 0°C

until $MgCl_2$ was completely dissolved. $TiCl_4$ (0.45 mL) was added into the PSA/$MgCl_2$/THF solution by dropwise at 0°C. The solution became yellow. After 2 h, *n*-hexane (50.0 mL) was slowly added into the solution by syringe. Yellow solid was precipitated from the solution. The residual solid was separated, washed several times until the liquid was colorless, and then dried at room temperature under vacuum for 4 h.

PSA/(*n*-Bu)MgCl/$TiCl_4$ catalyst

PSA/THF solution (20.0 mL) was added in a Schlenk flask (150 mL) and cooled down to 0°C. Then (*n*-Bu)MgCl (2.50 mL) was added into the solution by dropwise. The mixture was agitated for 1 h, followed by dropwise addition of $TiCl_4$ (0.35 mL) at 0°C. After 2 h, *n*-hexane (40.0 mL) was slowly added into the black colored mixture. Black yellow solid was separated from the mixture, washed several times by *n*-hexane until the liquid was colorless. The remaining slurry was dried under vacuum at room temperature for 4 h.

PSA/(*n*-Bu)$_2$Mg/$TiCl_4$ catalyst

As (*n*-Bu)$_2$Mg is stable in nonpolar solvent, we used PSA/toluene solution. PSA/toluene solution (20.0 mL) placed in a Schlenk flask (150 mL) was cooled down to 0°C. Then (*n*-Bu)$_2$Mg solution (1.20 mL) was added into the solution by dropwise. White sol-gel was formed. The mixture was stirred for 1 h, followed by dropwise addition of $TiCl_4$ (0.35 mL) at 0 °C. The black yellow mixture reacted for another 2 h, followed by slow addition of *n*-hexane (40.0 mL). The residual solid was separated, washed by hexane for several times, and then dried under vacuum at room temperature for 4 h.

Ethylene homopolymerization

Slurry ethylene homopolymerization were performed in a 1 L Büchi stainless steel autoclave reactor, equipped with mechanical stirrer, a mass flow meter, and a temperature control unit consisting of cooling water and an electric heater. The reactor was heated above 90°C for more than 2 h and repeatedly pressurized with nitrogen, purged and evacuated (<10 mbar) before polymerization. Then, the reactor temperature was set to the desired polymerization temperature. 350 mL *n*-heptane was added into the reactor. The catalyst was introduced into the reactor under nitrogen purging after the injection of appropriate TEA as cocatalyst. The stirring speed was set at 350 rpm. The polymerizations were performed at 0.50 MPa. At the end of the polymerizations, the reactor was rapidly vented, and the produced polymer was precipitated and washed with acidified (2 wt % hydrochloric acid) ethanol, filtered, and dried at 50°C under vacuum for 12 h.

Characterization

The XPS measurements were performed on a Kratos Axis Ultra DLD spectrometer using monochromatic a Al Kα souse ($h\nu = 1486.6$ eV). Spectra were taken at room temperature in high resolution modes for O 1s and Ti 2p. All of the binding energies at various peaks were calibrated using the binding energy of C 1s (284.8 eV). For every XPS spectra, we deconvoluted the experimental curve in a series of peaks which represent the contribution of the photoelectron emission from atoms in different chemical environments. FTIR measurements were performed on a Nicolet 5700 spectrometer. The crystallographic phases of the virginal PSA and the four catalysts were characterized by powder XRD (X'pert Pro MPO, Philip, the Netherlands) with Cu Kα (45 KV, 40 mA, graphite monocharomators). The scans were performed for diffraction angle from $2\theta = 5$ to 80° with a step of 0.2° and a counting time of 12 s. The samples were also observed by the Hitachi S-4700 SEM. Virginal PSA as well as the four catalysts was subjected to TGA using Mettler Toledo SDTA851 system. Samples of <10 mg were heated from 25 to 600°C at heating rate of 10°C/min in nitrogen atmosphere, and the corresponding weight loss was recorded. The magnesium content was determined by a titration method using the chelating agent, ethylenediamine tetraacetic acid. The content of titanium in the catalysts was determined by ultraviolet spectroscopy (UV). UV measurements were performed in 10-mm quartz glass cells on Unico UV-2102PC spectrophotometer. The intensity of the peak at 410 nm was used to quantify the titanium content.

RESULTS AND DISCUSSION

Spectroscopic properties of the catalysts

As shown in Figure 1, the O1s region of the X-ray photoelectron (XPS) spectrum from organic materials was wide. The oxygen peak of carbon materials is frequently deconvoluted into two components: one in the range 531.2–532.6 eV, attributed to oxygen doubly bound to carbon, and the other one in the range 532.8–533.1 eV, attributed to oxygen singly bound to carbon.[18] In this article, XPS Peak 4.1 software was used to deconvolute the high resolution O1s peak. The results are given in Table II. The chemical environments of the materials investigated here must be taken into consideration to understand the results. Peak 1 with higher BE value is assigned to C—O in the carboxyl group and peak 2 with

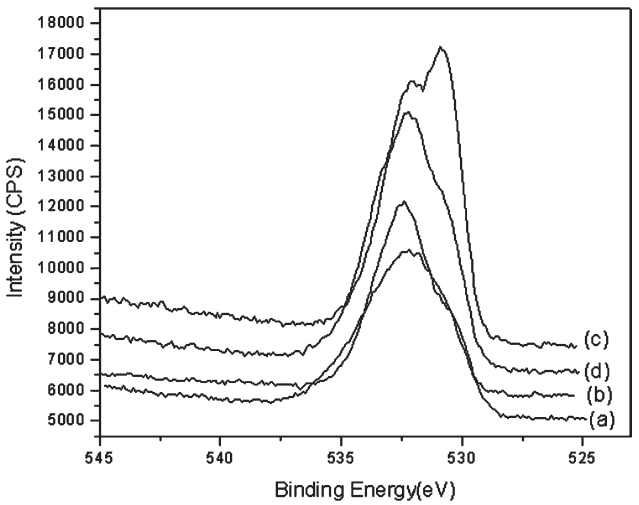

Figure 1 XPS survey spectra of O 1s recorded from the four catalysts (a) PT; (b) PMT; (c) PB1T and (d) PB2T.

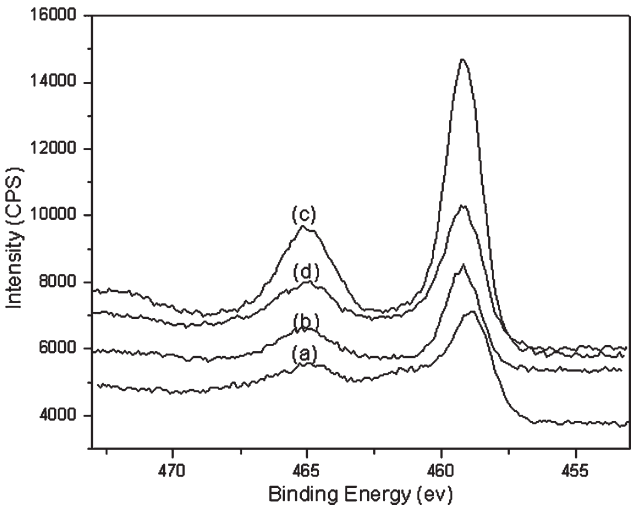

Figure 2 XPS survey spectra of Ti 2p recorded from the four catalysts (a) PT; (b) PMT; (c) PB1T and (d) PB2T.

lower BE value is owed to C=O in the carboxyl group.

As listed in Table II, the peak of O1s in PSA/$TiCl_4$ catalyst (PT) was deconvoluted into 534.0 eV and 535.7 eV. Similar result was found in case of PSA/$MgCl_2$/$TiCl_4$ catalyst (PMT). Generally, as the positive charge on the atom increases by formation of chemical bonds, BE will increase.[19] Thus, the deconvolution results with much higher BE values of O 1s in PT and PMT are assigned to species which are in electron-poor environments, probably due to the shift of electrons to Ti from —COOH groups. This indicates that $TiCl_4$ directly coordinate with —COOH groups in PT and PMT. In contrast, the BE of O 1s in PSA/(*n*-Bu)MgCl/$TiCl_4$ catalyst (PB1T) and PSA/(*n*-Bu)$_2$Mg/$TiCl_4$ catalyst (PB2T) clearly reduced, suggesting that no electron shifts to Ti atoms from —COOH groups. —COOH groups may attract excessive electrons from (*n*-Bu)MgCl or (*n*-Bu)$_2$Mg and lose the H atoms, resulting in electron-rich environments around O atoms. Thus, the BE of O 1s decreases in PB1T and PB2T. Based on these findings, it can be concluded that $TiCl_4$ has no direct chemical coordination with —COOH groups in PB1T and PB2T.

As shown in Figure 2, the BE values of Ti 2p in the four catalysts were higher than $TiCl_3$ (458.5 eV) and lower than $TiCl_4$ (459.8 eV).[20] The Ti 2p peak in the spectrum of PT was at 458.9 eV, which was lower than the Ti 2p peak at 459.2 eV of the other three catalysts. In general, as the negative charges on the atom increase by formation of chemical bonds, BE will decrease.[19,21] Lower Ti 2p BE value in PT illustrates that titanium atoms obtain more electronic charges in PT than in the other three catalysts. This can be explained by coordination between several —COOH groups with one $TiCl_4$ molecule.

Above all, the synthesis methods of polymer-supported catalysts exert a strong influence on the electron density around O and Ti atoms. $TiCl_4$ is supposed to directly coordinate with several —COOH groups in PT. Excessive electrons are shifted to $TiCl_4$ from —COOH, leading to electron-poor environment around O atoms and extremely high electron density around Ti atoms. Ti atoms in PMT also attract electrons from —COOH groups as well as in PT. However, the modification by $MgCl_2$ disables Ti to occupy electrons from several —COOH groups, leading to higher BE of Ti 2p in PMT than in PT. As (*n*-Bu)MgCl and (*n*-Bu)$_2$Mg react with —COOH, —COOMg- with strong chemical bond in O—Mg is formed, Ti is inhibited to directly coordinate with —COOH. Meanwhile, electron-rich environments around O appear in PB1T and PB2T due to the H atoms in —COOH groups has been drawn by these two magnesium compounds.

The FTIR spectra of virginal PSA and PSA-supported catalysts were studied to confirm the variations in chemical environment of the catalysts (Fig. 3). Typical adsorption band at 908.32 cm^{-1} attributed to —OH on carboxyl group[22] shifted to 877.47 cm^{-1} in the spectra of PT and PMT. However, this typical adsorption band almost disappeared in the spectra of PB1T and PB2T, indicating no —COOH present in the catalysts. —COOH may become —COOMg- due to the reaction between PSA and (*n*-Bu)MgCl or (*n*-Bu)$_2$Mg. This finding supports the results of XPS. Further, the characteristic band at

TABLE II
The Deconvolution Results of O 1s Survey Patterns

Catalyst	PT	PMT	PB1T	PB2T
Peak 1 (eV)	534.0	534.2	530.7	530.8
Peak 2 (eV)	535.7	535.8	532.3	532.5

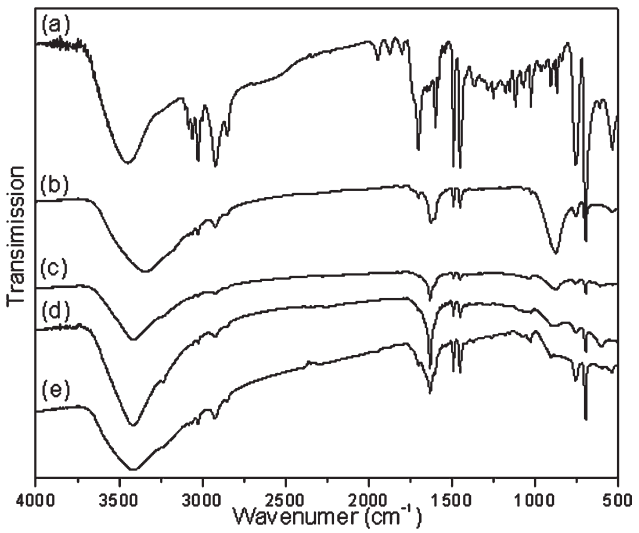

Figure 3 FTIR spectra of pure PSA and the four catalysts (a)PSA; (b) PT; (c) PMT; (d) PB1T and (e) PB2T.

1700 cm^{-1} assigned to the C=O stretching vibration[22] shifted to 1627 cm^{-1} after PSA supported catalysts. The other typical absorption-bands in the spectrum of virginal PSA,[23] including 757 and 698 cm^{-1} (the phenyl C—H out-of-plane bending and benzene out-of-plane ring bending), 2850–2950 cm^{-1} (aliphatic C—H stretching resonances), 1493 and 1452 cm^{-1} (the phenyl C=C stretching resonance), were much weaker or almost disappeared in the spectra of catalysts. This also confirms the chemical reactions between —COOH groups and $TiCl_4$ or magnesium compounds.

XRD measurements were performed to evaluate the effects of synthesis methods on the structure of polymer-supported catalysts. Spectra in Figure 4 indicate that the crystallinity of PSA obviously changes when it is used to support catalysts. The main peak of virginal PSA at 19° (2θ) with high intensity disappeared and a new peak at 8° (2θ) appeared in the pattern of PT, which may be associated with lattice disorder in PSA chains. In case of other catalysts, which were modified by magnesium agents, the main peak at 19° (θ) disappeared but no new peak appeared in the XRD patterns. This confirms that the coordination between magnesium agents and —COOH groups prevents PSA from recrystallization. As a result, PMT, PB1T, and PB2T are amorphous.

The morphology of the catalysts

XRD results imply that different particle morphologies may be observed in the four polymer-supported catalysts. To confirm the XRD results, SEM microphotographs of the polymer-supported $TiCl_4$ catalysts were taken. Overall, the catalyst particles were granular, having pores with different sizes and shapes. As observed in Figure 5(a), PT particles were highly compact with pores formed due to solvent evaporation, like the polymer membrane prepared by phase inversion method.[24,25] The polymer bulk in PT particles was tight. As shown in Figure 5(b–c), the catalyst particles were more disordered with the addition of magnesium compounds. On the other hand, regular first particles with interstices of considerable size were created in the modified catalysts. This means that the magnesium reagents are effective in disordering of polymer support structure. The coordination between PSA and magnesium compounds could change the chain arrangement and inhibit the recrystallinity of PSA.

However, the degree of disorder varies under different types of modifiers. The structure of PMT is found to be the most disordered, containing small thin slices with large interstice as wide as 2–3 μm. The interstice between the first particles of PB1T and PB2T, is much smaller than PMT. Especially, the first particles of PB2T are granular and more compacted. By correlation with the XPS results, it is confirmed that the modification mechanism of $MgCl_2$ is different from (*n*-Bu)MgCl and (*n*-Bu)$_2$Mg. $TiCl_4$ is hypothesized to be inserted into PSA and $MgCl_2$ which have been already weakly coordinated before. As a result, two-times reformation of chain structure takes place in PMT, leading to more intensively disordered catalyst particles. The chemical bonds between the other magnesium reagents and PSA are strong enough that $TiCl_4$ has no chance to take the place of (*n*-Bu)MgCl or (*n*-Bu)$_2$Mg to coordinate with PSA. Thus, only one structure reformation occurs in PB1T and PB2T.

TGA of the catalysts

The thermal decomposition behavior of virginal PSA, PT, PMT, PB1T, and PB2T were shown in

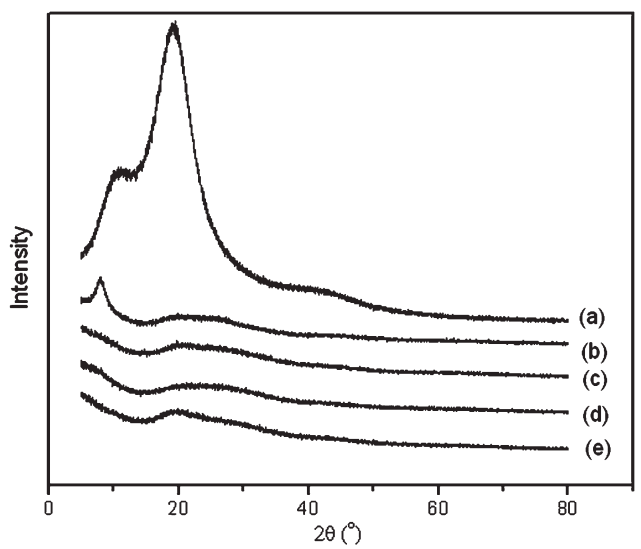

Figure 4 XRD patterns of virginal PSA and the four catalysts (a) PSA, (b) PT; (c) PMT; (d) PB1T and (e) PB2T.

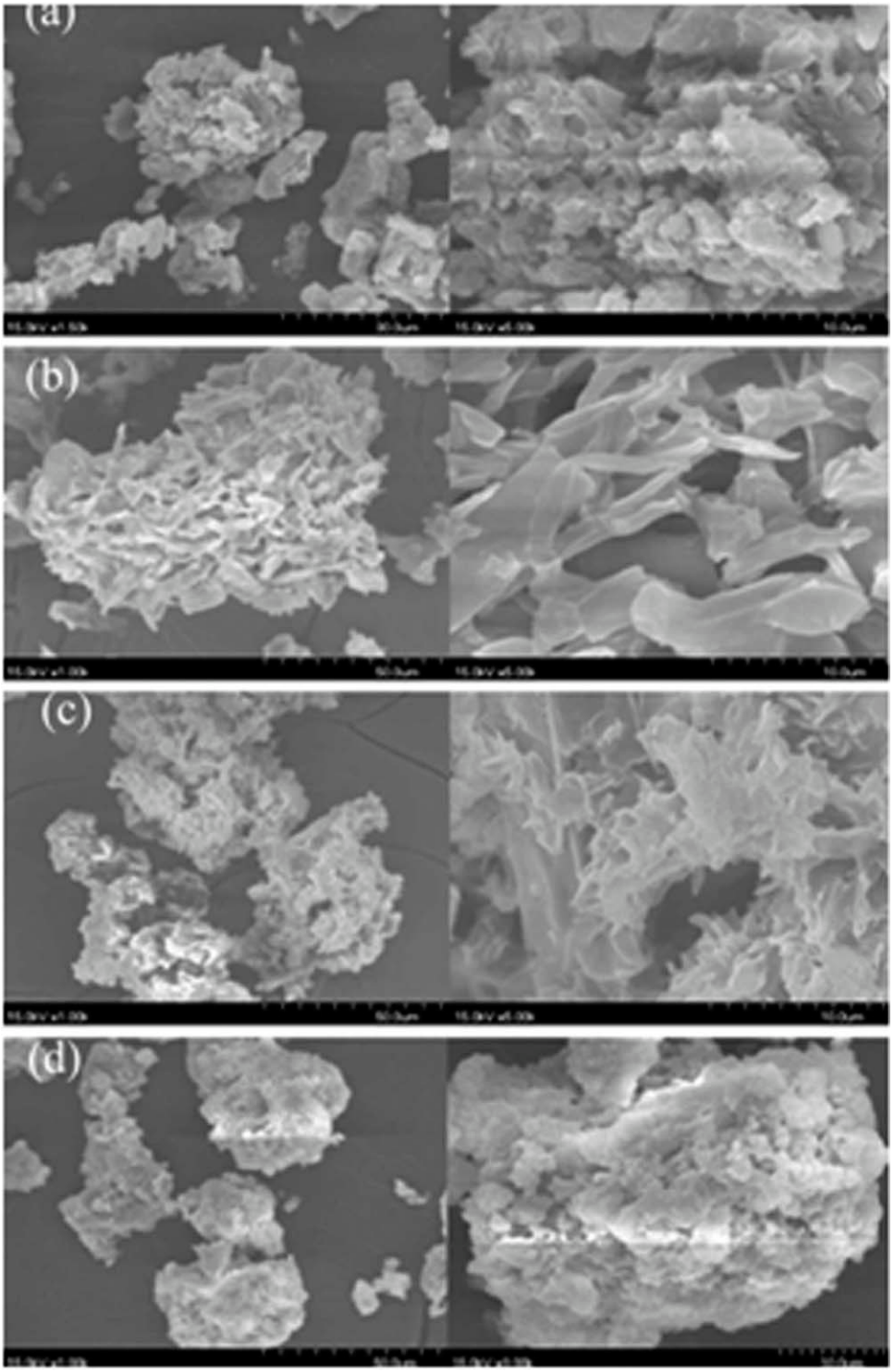

Figure 5 The morphologies of the four catalysts observed by SEM (a) PT; (b) PMT; (c) PB1T; (d) PB2T.

Figure 6. Weight losses and the temperature at maximum rate of decomposition were determined. The TG curves in Figure 6(1) illustrate that the virginal PSA and magnesium compounds-modified catalysts perform the similar tendency in the TGA process. They showed slow weight loss under 300°C and one distinctive loss between 350 to 450°C. The curve of PT presented two dramatic reductions in weight from 150 to 210°C and from 260 to 400°C, respectively. Differential thermogravimetric (DTG) curves of PMT, PB1T, and PB2T in Figure 6(2) showed the maximum decomposition rate at 412°C, as well as the virginal PSA. This implies that the PSA molecular structure is not destroyed during the catalyst

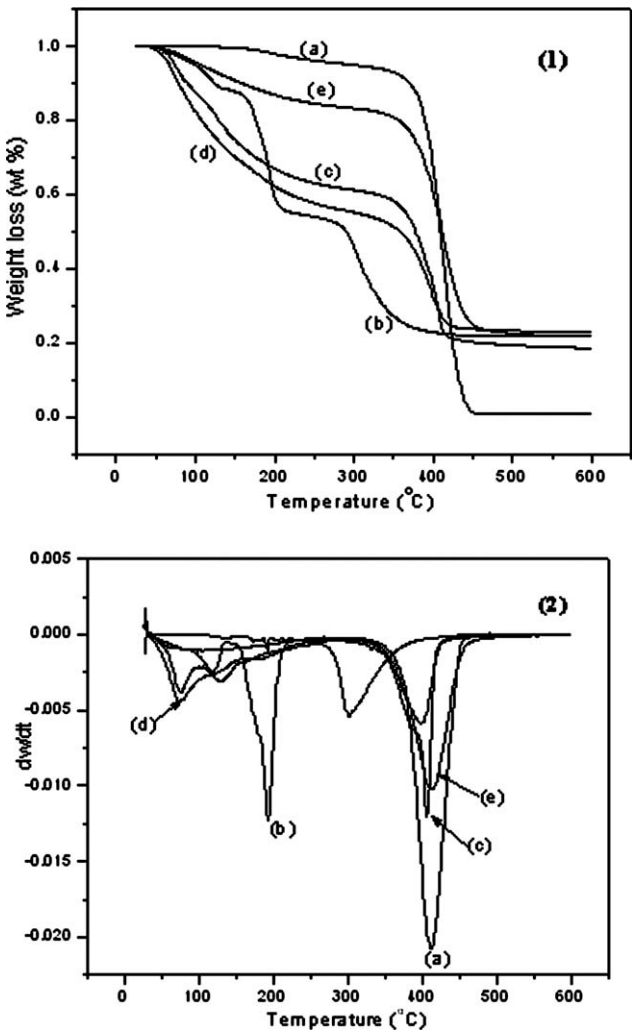

Figure 6 The TG results of the four catalysts (1)TG curves; (2) DTG curves: (a) PSA; (b) PT; (c) PMT; (d) PB1T; (e) PB2T.

supporting process. However, two peaks of thermal decomposition existed in the DTG curve of PT, at 193°C and 302°C, respectively, indicating a distinct deterioration in thermal stability occurs in PT. It was concluded previously that one $TiCl_4$ molecule could coordinate with several —COOH groups in PT. Random chain scissions of PSA is arose by such a fierce interaction causes. Random chain scissions can quickly cause serious destruction in polymer molecules and deterioration of thermal stability.[26]

Proposed structure of PSA-supported catalysts

The titanium and magnesium contents were listed in Table I. The supporting efficiency of Ti in PT was much lower than the other catalysts. The titanium content was only 0.102% in PT, confirming the conclusion that one $TiCl_4$ molecule can react with several carboxyl groups available on PSA molecules. The titanium content in the polymer-supported catalysts increased significantly when PSA was modified by magnesium compounds. This is caused by inhibition of direct and fierce coordination between $TiCl_4$ and PSA due to the presence of the magnesium reagents. Magnesium compounds are expected first to react with carboxyl groups on PSA, followed by anchoring of $TiCl_4$ molecules on the modified polymer support. Reasonably, stoichiometric relationship between $TiCl_4$ and —COOH would vary in PMT, PB1T, and PB2T.

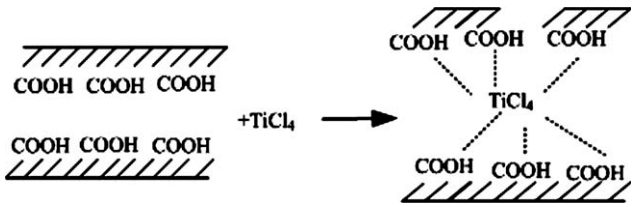

Scheme 1 The proposed structure of PT.

The previous detailed description of the results from XRD, FTIR, XPS, SEM, TGA, and element analysis is used to deduce the synthesis mechanisms of polymer-supported catalysts under various modification reagents. Four different synthesis mechanisms were provided in Schemes 1–4, respectively. The synthesis mechanism of PT is provided by Scheme 1. One $TiCl_4$ coordinates with multiple —COOH groups from one or several PSA chains. The PSA chains aggregate again after the addition of nonpolar solvent. As shown in Scheme 2–4, the magnesium compounds may coordinate with —COOH and insert into the PSA chains to prevent polymer aggregation. This leads to polymer gel with serious disordered structure and good dispersion of catalyst components. Diffusion of reactants to access active centers is enforced. As routine principles, $TiCl_4$ would coordinate with (*n*-Bu)MgCl to produce PB1T. $TiCl_4$ is also reduced when it coordinates with $(n\text{-Bu})_2Mg$ in preparation of PB2T. However, $TiCl_4$ takes the place

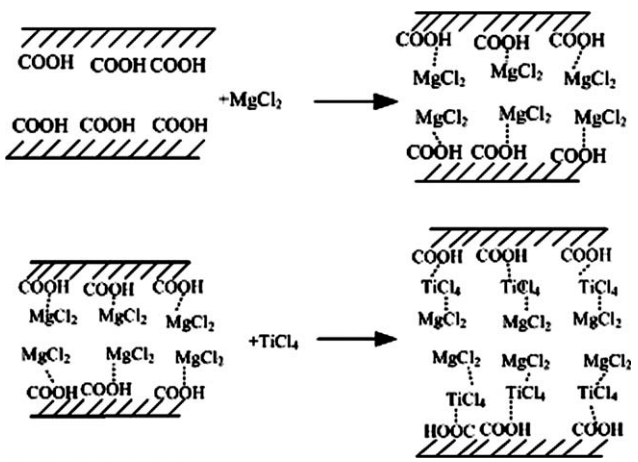

Scheme 2 The proposed structure of PMT.

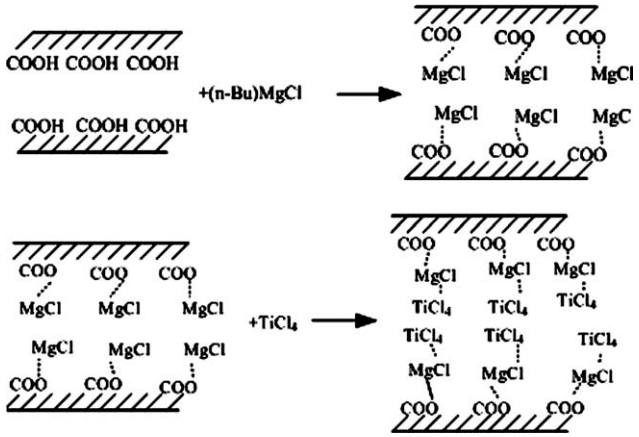

Scheme 3 The proposed structure of PB1T.

of $MgCl_2$ to coordinate with —COOH in the system of PMT due to the weaker chemical bonds between $MgCl_2$ and PSA. The proposed synthesis mechanisms are the main reactions in preparation processes of the catalysts. Some vice-product may also exist in the catalyst system.

Activity profiles in ethylene homopolymerization

Figure 7 shows the polymerization profiles at 75°C. The catalyst activity was calculated as the mass of resulting polymer divided by the grams of metal per minute. Overall, the catalyst activity is enhanced by magnesium compounds in the following order: $MgCl_2$ > (*n*-Bu)MgCl > $(n\text{-Bu})_2Mg$ > no modifier. PT shows the lowest activity because of the low Ti content and large numbers of ineffective active site O—Ti. PMT showed the highest initial and average activity among the four catalysts. Furthermore, PMT reached the maximum activity in 15 min, much faster than the other catalysts. Two aspects are assigned to the good performance of PMT. First, modification with $MgCl_2$ provides a beneficial electron environment for $TiCl_4$. Second, the most disordered structure of catalyst with large pore size

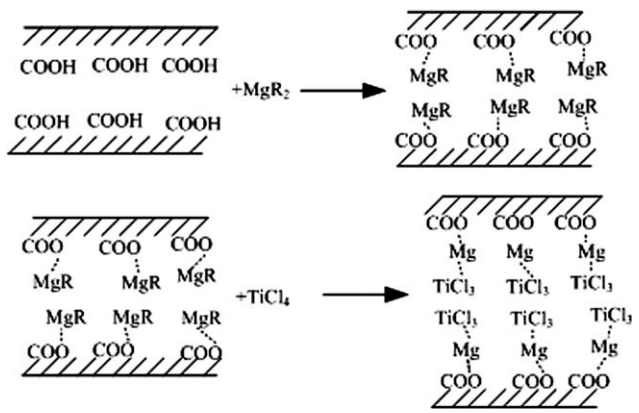

Scheme 4 The proposed structure of PB2T.

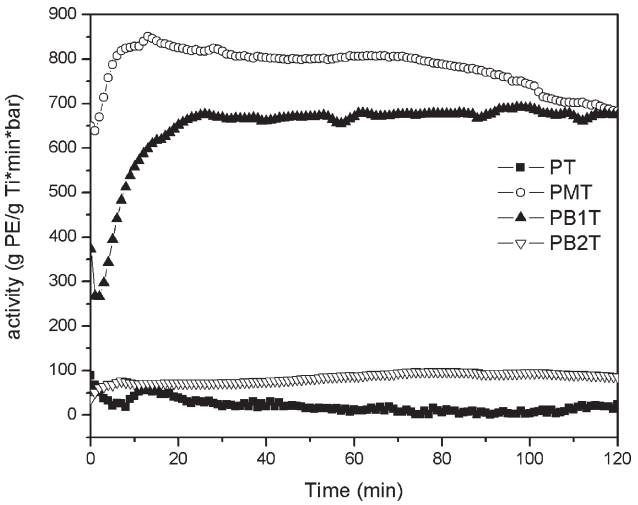

Figure 7 Activity profiles of ethylene polymerization at 75°C.

inside particles enhances the diffusion of reactants to access the interior active centers. The less degree of disorder and smaller pore size in P1BT allow its activity rise slowly to the top and then keep constant until the termination of polymerization. The activity of PB2T slowly increased during the whole polymerization process. Although much ethylene was consumed in the ethylene polymerization of PB2T, the catalyst activity based on per gram Ti was low due to the high titanium content in PB2T. Over-reduced $TiCl_4$ owing to the strong reduction ability of $(n\text{-Bu})_2Mg$[27] and inadequate surface area in the compacted catalyst particles are attributed to the low activity of PB2T.

Ethylene polymerizations were also performed at different temperatures, including 50 and 85°C. Although the average catalyst activity is still enhanced by magnesium compounds in the following order: $MgCl_2$ > (*n*-Bu)MgCl > $(n\text{-Bu})_2Mg$ > no modifier, the shape of activity profiles is varied. PT shows low activity at any temperature. The difference in the activity of the other three modified catalysts becomes more significant with increasing polymerization temperatures. PB2T shows the highest activity at 50°C while PMT and PB1T have the maximum activity at 75°C. The degree of the swelling of polymer support and the nature of active sites are varied at different temperature. Both of them can directly influence the performance of the catalysts (Figs. 8 and 9). A more thorough discussion of ethylene polymerizations under various conditions will be provided in a forthcoming paper.

CONCLUSIONS

Four PSA-supported $TiCl_4$ catalysts modified by various magnesium reagents were synthesized and

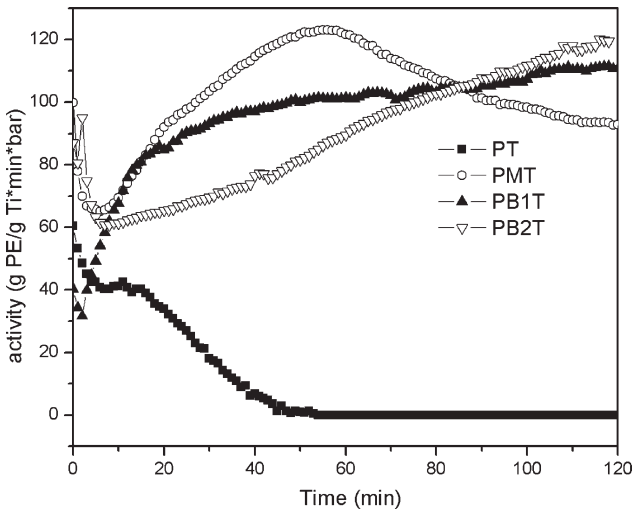

Figure 8 Activity profiles of ethylene polymerization at 50°C.

used for ethylene polymerization. Chemical environments and physical structures of the synthesized catalysts were investigated. According to these results, the mechanisms of reactions between polymer support, magnesium compounds and $TiCl_4$ were proposed. It was novel to find that $TiCl_4$ could substitute $MgCl_2$ to coordinate with —COOH in the synthesis of PSA/$MgCl_2$/$TiCl_4$. However, $TiCl_4$ had no chance to access —COOH groups in preparation of PSA/(*n*-Bu)MgCl/$TiCl_4$ and PSA/(*n*-Bu)$_2$Mg/$TiCl_4$ due to the strong chemical bonds between O and Mg in —COOMg-. On the other hand, the modification by magnesium compounds disordered the chain structure of PSA. The disordered degree was depended on the type of magnesium compounds. Ethylene polymerization results indicated that the polymer-supported catalyst activity was enhanced by magnesium compounds in the following order: $MgCl_2$ > (*n*-Bu)MgCl > (*n*-Bu)$_2$Mg > no modifier.

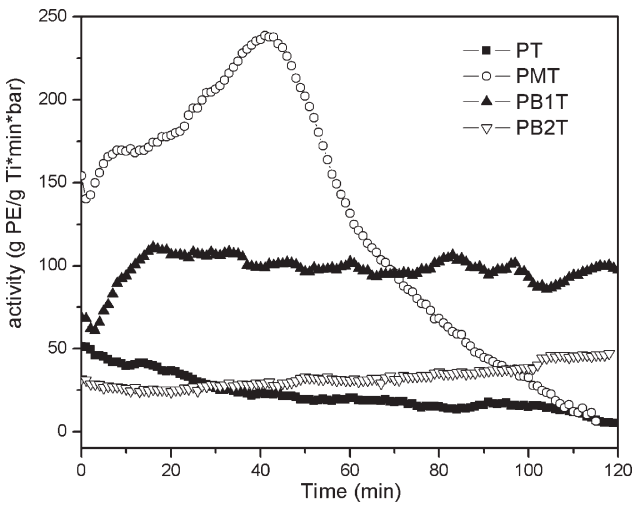

Figure 9 Activity profiles of ethylene polymerization at 85°C.

The performance of the catalysts was varied at different polymerization temperatures. The chemical environments around Ti atoms and physical structures of the polymer-supported catalysts are the reasons for different performance in the ethylene polymerization process. For understanding more about the polymer-supported catalysts, a more thorough investigation of ethylene polymerizations under various conditions will be discussed in the following work.

References

1. Pomogailo, A. D. Kinet Katal 2004, 45, 61.
2. Scherrington, D. C. J Polym Sci Part A: Polym Chem 2001, 39, 2364.
3. Yu, G.; Chen, H.; Zhang, X.; Jiang, Z.; Huang, B. J Polym Sci Part A: Polym Chem 1996, 34, 2237.
4. Gupta, V.; Vinod, C. P.; Kulkarni, G. U.; Lahiri, G. K.; Maity, N.; Bhaduri, S. Curr Sci 2005, 88, 1162.
5. Dioos, B. M. L.; Vankelecom, I. F. J.; Jacobs, P. A. Adv Synth Catal 2006, 348, 1413.
6. Sun, L.; Hsu, C. C.; Bacon, D. W. J. J Polym Sci Part A: Polym Chem 1994, 32, 2127.
7. Sun, L.; Hsu, C. C.; Bacon, D. W. J. J Polym Sci Part A: Polym Chem 1994, 32, 2135.
8. Mteza, S. B.; Hsu, C. C.; Bacon, D. W. J Polym Sci Part A: Polym Chem 1996, 34, 1693.
9. Jerico, S.; Schuchardt, U.; Joekes, I.; Kaminsky, W.; Noll, A. J Mol Catal A: Chem 1995, 99, 167.
10. Kaur, S.; Singh, G.; Kothari, A. V.; Gupta, V. K. J Polym Sci Part A: Polym Chem 2008, 46, 7299.
11. Roscoe, S. B.; Gong, C.; Frechet, J. M. J.; Walzer, J. F. J Polym Sci Part A: Polym Chem 2000, 38, 2979.
12. Nishida, H.; Uozumi, T.; Arai, T.; Soga, K. Macromol Rapid Commun 1995, 16, 821.
13. Bouilhac, C.; Cramail, H.; Cloutet, E.; Deffieux,A.; Taton, D. J Polym Sci Part A: Polym Chem 2006, 44, 6997.
14. Shi, L.; Qin, Y.; Cheng, W.; Chen, H.; Tang, T. Polymer 2007, 48, 2481.
15. Pomogailo, A. D. Polym Sci Ser A 2008, 50, 1204.
16. Stork, M.; Koch, M.; Klapper, M.; Müllen, K.; Gregorius, H.; Rief, U. Macromol Rapid Commun 1999, 20, 210.
17. Barrett, A. G. M.; de Miguel, Y. R. Chem Commun 1998, 19, 2079.
18. Pamula, E.; Rouxhet, P. G. Carbon 2003, 41, 1905.
19. Vicherman, J. C.; Gilmore, I. S. Surface Analysis: The principal Techniques, 2nd ed.; United Kingdom, Wiley, 2009, p 55.
20. Sleigh, C.; Pijpers, A. P.; Jaspers, A.; Coussens, B.; Meier, R. J. J Electron Spectrosc 1996, 77, 41.
21. Niemantsverdriet, J. W. Spectroscopy in Catalysis: An Introduction; Wiley-VCH Verlag GmbH & Co. KGaA: Weiheim, 1993, p 39.
22. Liu, Z. L.; Ding, Z. H.; Yao, K. L.; Tao, J.; Du, G. H.; Lu, Q. H.; Wang, X.; Gong, F. L.; Chen, X.; J Magn Magn Mater 2003, 265, 98.
23. Du, L.; Li, W.; Fan, L.; Jiang, B.; Wang, J.; Yang, Y.; Liao, Z. J Appl Polym Sci 2010, 118, 1743.
24. Matsuyama, H.; Yano, H.; Maki, T.; Teramoto, M. J Membr Sci 2001, 194, 157.
25. Stropnik, C.; Germic, L.; Zerjal, B. J Appl Polym Sci 1996, 61, 1821.
26. Beyler, C. L.; Custer, R. P.; Walton, W. D.; Jr. Watts, J. M.; Drysdale, D.; Jr. Hall, J. R.; Dinenno, P. J. In the SFPE Handbook of Fire Protection Engineering, 2nd ed.; National Fire Protection Association, Society of Fire Protection Engineers in Quincy, Mass, Boston, Mass, 1995, pp 1–123.
27. Malpass, D. B. Introduction to Industrial Polyethylene: Properties, Catalysts, and Process; John Wiley & Sons, Inc.: Hoboken, 2010, p 52.